View Article Online / Journal Homepage / Table of Contents for this issue

ChemComm

This article is part of the

Porphyrins & Phthalocyanines

web themed issue

Guest editors: Jonathan Sessler, Penny Brothers and
Chang-Hee Lee

All articles in this issue will be gathered together
online at
www.rsc.org/porphyrins

ChemComm

Dynamic Article Links

Cite this: *Chem. Commun.*, 2012, **48**, 5512–5514

www.rsc.org/chemcomm

COMMUNICATION

Controlled growth of narrowly dispersed nanosize hexagonal MOF rods from Mn(III)–porphyrin and In(NO_3)$_3$ and their application in olefin oxidation†‡

Da Hee Lee,[a] Sundol Kim,[a] Min Young Hyun,[b] Jin-Yeon Hong,[c] Seong Huh,[c] Cheal Kim*[b] and Suk Joong Lee*[a]

Received 14th February 2012, Accepted 11th April 2012
DOI: 10.1039/c2cc31075a

A new class of narrowly dispersed nanosize hexagonal MOF rods from Mn(III)–porphyrin and In(III) was obtained. The length of MOF rods was controlled by simple change of reaction times. Furthermore, the oxidation of styrene has been successfully demonstrated with Mn(III)–porphyrin MOF rods and their reusability has been also tested.

Metal–organic frameworks (MOFs), resulting from the self-assembly of metal complexes and organic linkers, have received a great deal of attention due to their potential applications in catalysis, gas storage, molecular recognition, separation and optics.[1] Recently, nano- and micro-scale MOFs (nMOFs or mMOFs) have been reported with promising applications.[2] They provide various features like the advantages of nanomaterials in addition to the properties of MOFs.[3] Furthermore, they often show novel and/or enhanced properties in applications such as gas storage,[4] separation,[5] drug delivery,[6] biosensing and imaging,[7] and catalysis.[8] However, the fabrication of nMOFs and mMOFs is still a very challenging task because of the dearth of information and knowledge regarding the critical factors required for the precise control of these materials, even though a variety of nano- and micro-scale MOFs showing different morphologies can be successfully obtained by controlling the growth conditions of crystals.[9] Specially, the translation of their building blocks into well-defined MOF particles, therefore, tuning their properties at the building block level remains still quite challenging.[10]

As a good building block, metalloporphyrin often shows its unique functions in a wide range of molecular architectures, such as molecular boxes, self-assembled arrays and coordination polymers, and MOFs with various applications in gas storage,[11] catalysis,[12] and separation.[13] In particular, Mn(III) and Fe(III) mediated porphyrin derivatives are often used to mimic the remarkable behavior of enzymes, that is the selective oxidation of olefins. Unfortunately, when used as homogeneous catalysts, they often suffer from quick degradation such as ligand oxidation or μ-oxo dimer formation.[14] Therefore, immobilization and site-isolation of homogeneous catalysts on organic polymers, inorganic supports and MOFs to screen out the side reactions has become one of the most promising fields in current chemistry.[15]

In this spirit, we would like to describe herein the preparation and properties of length-controlled nano- and microsize hexagonal MOF rods from Mn(III)–porphyrin biscarboxylic acid and In(NO_3)$_3$, and their catalytic behaviour in olefin oxidation as a heterogeneous catalyst.

Mn(III)–porphyrin bis-carboxylic acid **1** has been prepared according to the modified literature procedure that is the condensation reaction between dipyrrolemethane and aldehyde followed by deprotection of ethyl groups and metallation with $MnCl_2$ (Scheme S1 in ESI‡).[16] In order to make the best use of bis-carboxylic groups of the Mn(III)–porphyrin, In(NO_3)$_3$ was chosen to assemble networks because In^{3+} is well known to allow strong interactions with carboxylates to generate stable coordinative networks.[17] Therefore, using a high temperature stirring method,[18] a solution of **1** (3.134 mg) and In(NO_3)$_3$ (1.949 mg) in 0.45 mL of anhydrous DMF was vigorously stirred at 120 °C for approximately 2, 5, 10, 30 and 60 min, respectively, and translucent dark brown suspensions were obtained after cooling. Analysis by scanning electron microscopy (SEM) reveals these suspensions to be collections of fairly uniform hexagonal rods which show systematically modulated lengths by adjusting reaction times (Fig. 1). Presumably, when the reaction is initiated in DMF at 120 °C, crystalline seeds are generated and they continue to grow until they are held in a solution phase. As they are cooled down, these nanocrystalline rods become less soluble and precipitate from the DMF medium. The lengths of the resulting rods are controlled by the ability of the solution to support the particles at high temperature, leading to narrowly dispersed Mn(III)–porphyrin MOF rods.[19]

---

[a] *Dept. of Chemistry, RINS, Korea University, 5 Anam-dong, Sungbuk-gu, Seoul 136-701, Korea. E-mail: slee1@korea.ac.kr; Tel: +82 2-924-3145*
[b] *Dept. of Fine Chemistry, Seoul National University of Science and Technology, Seoul 139-743, Korea. E-mail: chealkim@seoultech.ac.kr*
[c] *Dept. of Chemistry and Protein Research Center for Bio-Industry, Hankuk University of Foreign Studies, Yongin 449-791, Korea*

† This article is part of the ChemComm 'Porphyrins and phthalocyanines' web themed issue.

‡ Electronic supplementary information (ESI) available: Complete experimental details of syntheses, compound characterization, catalysis details, additional SEM images, EDX, PXRD patterns, TGA, and adsorption–desorption isotherms. See DOI: 10.1039/c2cc31075a

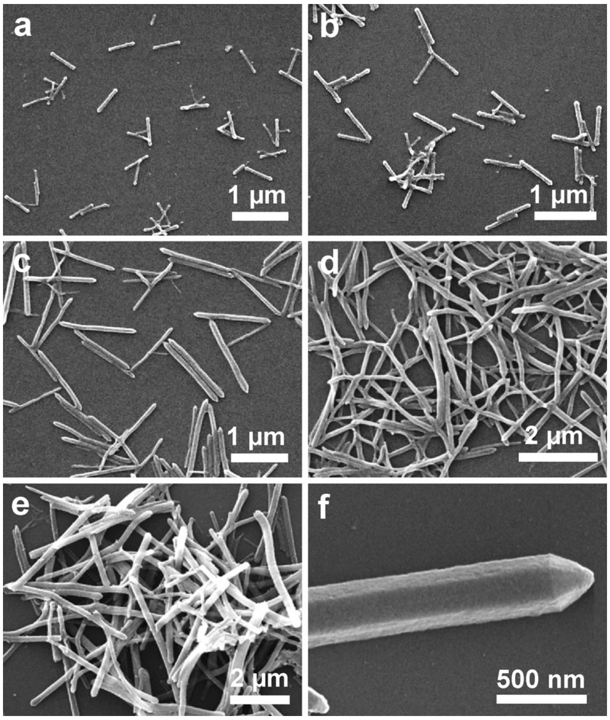

Fig. 1 SEM images of hexagonal MOF rods with different lengths obtained from Mn(III)–porphyrin **1** and In$(NO_3)_3$ at 120 °C at various reaction times; (a) 2, (b) 5, (c) 10, (d) 30, and (e) 60 min, and (f) a magnified image of a MOF rod grown from 60 min of reaction at 120 °C.

Therefore, we have increased the reaction time to maximize the solubility of porphyrin MOF rods in DMF during the crystal growth. The longer reaction time may extend their retention time in solution and hold the growth of particles to larger objects while maintaining the narrow distribution. Upon allowing the reaction for 60 min at 120 °C and cooling down to room temperature, narrowly dispersed hexagonal MOF rods are obtained with ~3.6 µm in length (Fig. 1e). Remarkably, when the reaction time was diversified, the lengths of hexagonal MOF rods changed dramatically. As shown in Fig. 1, narrowly dispersed MOF rods with lengths ranging from 0.5 ± 0.2 to 3.6 ± 1.2 µm can be obtained. However, the widths of these MOF rods are also increased from ~70 to ~350 nm. Although obtaining suitable single crystals for X-ray structure analysis has not been successful, these materials exhibit remarkably the same powder X-ray diffraction (PXRD) patterns, indicating the identical unit cells despite their different lengths (Fig. S2 in ESI‡).

Similar behaviors have been observed when the reactions have been carried out at 100 °C and 80 °C, respectively. At 100 °C, the lengths of hexagonal MOF rods ranging from 0.3 ± 0.2 to 2.5 ± 0.7 µm can be obtained over a reaction time range of 5 to 60 min (Fig. S3 in ESI‡). However, no MOF rods were observed for the 2 min reaction (Fig. S3a in ESI‡). Similarly, when the reactions were carried out at 80 °C, the lengths of MOF rods ranged from 0.4 ± 0.1 to 1.6 ± 6.0 µm (Fig. S4 in ESI‡) and no MOF rods were observed for the 2 and 5 min reactions, respectively (Fig. S4a and b in ESI‡). Presumably, crystalline seeds require longer reaction time to grow and require high reaction temperature until they are retained in a solution phase and grow into longer rods.

Furthermore, when moderately diluted reactions (9 mL instead of 4.5 mL of DMF) were carried out at 120 °C, the lengths of MOF rods became greater than 5.5 µm despite the variation in reaction times, except for the reaction that was carried out for 2 min which gave a wide range of lengths from 50 nm to 400 nm (Fig. S5 in ESI‡). Indeed the solubility of porphyrin MOF rods becomes highly increased under this diluted condition.

To investigate the thermal stability of MOF rods, thermogravimetric analysis (TGA) of the samples obtained at various reaction times at 120 °C was performed. The TGA curves show an initial weight loss due to solvent liberation and a high thermal stability up to 280 °C. They show continuous weight loss in the range from 280 °C to 800 °C due to the decomposition of frameworks (Fig. S7 in ESI‡). Furthermore, the sample of MOF rods obtained from 10 min of reaction at 120 °C was chosen to study their gas sorption properties. Its volumetric gas sorption measurements were carried out using N_2, CO_2, and H_2 at 77 K, 196 K, and 77 K, respectively. As shown in Fig. S8 in ESI‡, the N_2 adsorption isotherm reveals a surface area of 77.7 $m^2\ g^{-1}$ and an uptake value of 85.1 $cm^3\ g^{-1}$, while the sorption of H_2 and CO_2 shows uptake values of 53.9 and 53.8 $cm^3\ g^{-1}$, respectively. Perhaps, the relatively smaller surface area and gas uptakes are attributed to the framework collapse during the $CHCl_3$-exchange and/or evacuation processes. This framework collapse was identified from the PXRD pattern taken after the gas sorption measurements, showing an almost complete loss of crystallinity. However, when an amorphous solid is immersed in DMF, it changes to somewhat original crystalline phase, which was detected from PXRD patterns (Fig. S9 in ESI‡). This flexible framework may provide pore structures that are suitable for the given guest molecules.[20]

With the readily accessible Mn(III)–porphyrin catalyst on board, the MOF rods grown from 10 min reaction at 120 °C have been selected and tested for their catalytic activity in oxidation of aromatic olefins. The catalyst was prepared by immerging in CH_2Cl_2 for 24 h followed by a brief drying to prevent complete decomposition of their framework. Styrene epoxidation using this MOF rod catalyst and its homogeneous counterpart Mn(III)–porphyrin bis-carboxyethylester **2** revealed

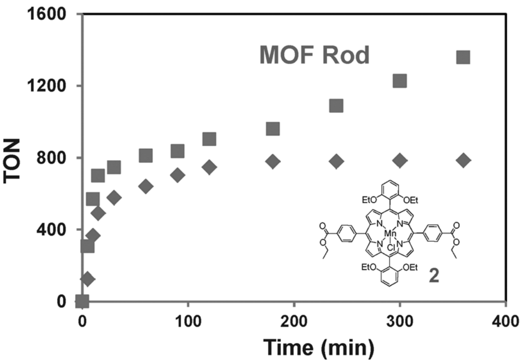

Fig. 2 Comparison of TONs and catalytic stability of the MOF rods obtained from 10 min of reaction at 120 °C and homogeneous catalyst {5,15-bis(4-carboxyethylphenyl)-10,20-bis[2,6-diethoxyphenyl]porphyrinato}manganese(III) chloride **2** (molar ratio of styrene : oxidant : catalyst = 2000 : 1000 : 1, CH_2Cl_2 5 mL). 2-*tert*-Butylsulfonyliodosylbenzene was used as an oxidant (see ESI‡ for detailed catalysis conditions).

Table 1 Investigation of the recyclability of MOF rods[a]

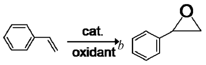

Number of catalytic cycles	1	2	3	4	5
TON[c]	888	900	893	891	885

[a] Reaction conditions; styrene: 0.48 mmol, oxidant: 0.24 mmol, MOF rods: 0.24×10^{-3} mmol (2000 : 1000 : 1), CH_2Cl_2: 1 mL, reaction time: 2 h, rt. [b] Oxidant: 2-*tert*-butylsulfonyliodosylbenzene. [c] Determined by GC with undecane as an internal standard (2000 eq.).

a dramatic change in the turnover number (TON). In addition, the catalyst lifetime was dramatically extended from approximately 2 hours to greater than 6 hours because of the formation of Mn(III)–porphyrin in the MOF (Fig. 2). Self-degradation of catalysts by oxo-bridged dimer formation was successfully blocked by the immobilization of catalysts through the MOF strategy.[14] Furthermore, the MOF rods obtained after the reaction were separated by centrifugation and reused 5 times. As shown in Table 1, they show outstanding reusability without losing their catalytic activity significantly and the morphology of MOF rods has been retained after the oxidation (Fig. S10 in ESI‡). Furthermore, the active catalyst species did not leach into solution which was confirmed by performing the reaction with a solution prepared by filtrating a MOF rod suspension in MC after shaking for 24 h. We next investigated the influence of the size of MOF rods on the catalytic activities because the active catalytic sites may be located only on the external surface which is affected by the size of crystallites. As shown in Table 2, the TONs decreased upon increasing the size of MOF rods. The same behaviors have been observed when the relatively bigger substrates (*Z*)- and (*E*)-stilbenes are used. These observations suggest that most of the catalytic reactions occur on the external surface of MOF rods and the number of active catalytic sites varies with the size of crystallites. However, the size-selectivity has been also observed. For example, the TONs of reactions with (*E*)-stilbene decreased significantly compared to those with styrene cases, while the TONs of the reactions with (*Z*)-stilbene decreased moderately. This observation suggests that the MOF rods provide non-negligible size of cavities which do not allow the bigger substrate to enter but the smaller one, albeit in a significantly changed TONs. Although the MOF rods show outstanding catalytic activity together with long lifetime, they allow most of the reactions to occur on their external surfaces and provide non-negligible size of cavities where smaller substrates may enter and react.

In summary, we have developed a new class of narrowly dispersed nanosize hexagonal MOF rods from a Mn(III)–porphyrin and In(III). The length of MOF rods has been easily controlled from nano- to micrometer by a simple change of reaction times. PXRD patterns show that these particles have an identical unit cell regardless of a wide range of length distributions. Furthermore, the oxidation of styrene has been successfully demonstrated with Mn(III)–porphyrin MOF rods. The catalytic activity and lifetime were dramatically improved and the self-degradation of catalysts was successfully blocked by the immobilization of Mn(III)–porphyrin through MOF formation. In addition, MOF rods show good recyclability without losing their catalytic activity after 5 runs.

Table 2 TONs of various olefin oxidations with MOF rods obtained at 120 °C at various reaction times[a]

	2 min	5 min	10 min	30 min	60 min
Styrene	1054	1003	957	926	905
(*Z*)-Stilbene	899	881	861	842	821
(*E*)-Stilbene	615	614	596	563	528

[a] Reaction conditions; olefin: 0.48 mmol, oxidant (2-*tert*-butylsulfonyliodosylbenzene): 0.24 mmol, MOF rods: 0.24×10^{-3} mmol (2000 : 1000 : 1), CH_2Cl_2: 1 mL, reaction time: 3 h, rt.

The authors acknowledge the financial support from the Korea Research Foundation Program (No. 20110004727) and Priority Research Centers Program (NRF 2011-0018396) through the National Research Foundation of Korea (NRF) funded by the Ministry of Education, Science and Technology (MEST).

Notes and references

1 (*a*) E. W. Berg and A. Alam, *Anal. Chim. Acta*, 1962, **27**, 454; (*b*) X. Zhao, B. Xiao, A. J. Fletcher, K. M. Thomas, D. Bradshaw and M. J. Rosseinsky, *Science*, 2004, **306**, 1012.
2 M. Oh and C. A. Mirkin, *Nature*, 2005, **438**, 651.
3 (*a*) A. Carne, C. Carbonell, I. Imaz and D. Maspoch, *Chem. Soc. Rev.*, 2011, **40**, 291; (*b*) A. M. Spokoyny, D. Kim, A. Sumrein and C. A. Mirkin, *Chem. Soc. Rev.*, 2009, **38**, 1218.
4 (*a*) S. Diring, S. Furukawa, Y. Takashima, T. Tsuruoka and S. Kitagawa, *Chem. Mater.*, 2010, **22**, 4531; (*b*) Z. Xin, J. Bai, Y. Pan and M. J. Zaworotko, *Chem.–Eur. J.*, 2010, **16**, 13049.
5 L. G. Qiu, Z. Q. Li, Y. Wu, W. Wang, T. Xu and X. Jiang, *Chem. Commun.*, 2008, 3642.
6 P. Horcajada, T. Chalati, C. Serre, B. Gillet, C. Sebrie, T. Baati, J. F. Eubank, D. Heurtaux, P. Clayette, C. Kreuz, J.-S. Chang, Y. K. Hwang, V. Marsaud, P.-N. Bories, L. Cynober, S. Gil, G. Ferey, P. Couvreur and R. Gref, *Nat. Mater.*, 2010, **9**, 172.
7 K. M. L. Taylor-Pashow, J. D. Rocca, R. C. Huxford and W. Lin, *Chem. Commun.*, 2010, **46**, 5832.
8 (*a*) D. Jiang, T. Mallat, F. Krumeich and A. Baiker, *Catal. Commun.*, 2011, **12**, 602; (*b*) L. H. Wee, S. R. Bajpe, N. Janssens, I. Hermans, K. Houthoofd, C. E. A. Kirschhock and J. A. Martens, *Chem. Commun.*, 2010, **46**, 8186.
9 L. Ma, C. Abney and W. Lin, *Chem. Soc. Rev.*, 2009, **38**, 1248.
10 S.-W. Kim, M. Kim, W. Y. Lee and T. Hyeon, *J. Am. Chem. Soc.*, 2002, **124**, 7642.
11 (*a*) J. Xia, S. Yuan, Z. Wang, S. Kirklin, B. Dorney, D.-J. Liu and L. Yu, *Macromolecules*, 2010, **43**, 3325; (*b*) X.-S. Wang, L. Meng, Q. Cheng, C. Kim, L. Wojtas, M. Chrzanowski, Y.-S. Chen, X. P. Zhang and S. Ma, *J. Am. Chem. Soc.*, 2011, **133**, 16322.
12 (*a*) M.-H. Xie, X.-L. Yang and C.-D. Wu, *Chem. Commun.*, 2011, **47**, 5521; (*b*) M.-H. Xie, X.-L. Yang, C. Zou and C.-D. Wu, *Inorg. Chem.*, 2011, **50**, 5318.
13 C. Y. Lee, O. K. Farha, B. J. Hong, A. A. Sarjeant, S. T. Nguyen and J. T. Hupp, *J. Am. Chem. Soc.*, 2011, **133**, 15858.
14 M. L. Merlau, M. d. P. Mejia, S. T. Nguyen and J. T. Hupp, *Angew. Chem., Int. Ed.*, 2001, **40**, 4239.
15 (*a*) N. E. Leadbeater and M. Marco, *Chem. Rev.*, 2002, **102**, 3217; (*b*) D. E. De Vos, M. Dams, B. F. Sels and P. A. Jacobs, *Chem. Rev.*, 2002, **102**, 3615.
16 S. J. Lee, K. L. Mulfort, X. Zuo, A. J. Goshe, P. J. Wesson, S. T. Nguyen, J. T. Hupp and D. M. Tiede, *J. Am. Chem. Soc.*, 2008, **130**, 836.
17 (*a*) S. Yang, X. Lin, A. J. Blake, G. S. Walker, P. Hubberstey, N. R. Champness and M. Schroder, *Nat. Chem.*, 2009, **1**, 487; (*b*) G. Zhou, Y. Yang, R. Fan, W. Cao and B. Yang, *CrystEngComm*, 2012, **14**, 193.
18 E.-H. Ryu, J. H. Lee, Y. S. Lee, J.-M. Gu, S. Huh and S. J. Lee, *Inorg. Chem. Commun.*, 2011, **14**, 1648.
19 S. J. Lee, J. T. Hupp and S. T. Nguyen, *J. Am. Chem. Soc.*, 2008, **130**, 9632.
20 S. Hasegawa, S. Horike, R. Matsuda, S. Furukawa, K. Mochizuki, Y. Kinoshita and S. Kitagawa, *J. Am. Chem. Soc.*, 2007, **129**, 2607.